

STATUS OF NSLS-II*

F. Willeke[#] for the NSLS-II Team

Brookhaven National Laboratory, Upton, NY 11973-5000, U.S.A.

Abstract

NSLS-II [1], the new 3 GeV 3rd generation light source presently under construction at Brookhaven National Laboratory will provide ultra-bright synchrotron radiation of 10^{21} photons·s⁻¹·mm⁻²·mrad⁻²·0.1%BW⁻¹@ 2keV and high photon flux of 10^{15} photons·s⁻¹·0.1%BW⁻¹. The facility will support a minimum of 60 beamlines. Construction started in 2009 and commissioning is expected to be completed in 2014. This report will provide a description of the NSLS-II design and will summarize the status of the construction project.

INTRODUCTION

NSLS, the National Synchrotron Light Source at BNL, is a very productive synchrotron light facility in its 4th decade of operation. While the strong scientific program is on-going, state-of-the-art accelerator technology can provide 10^4 times brighter photon beams than what is currently provided by NSLS. This large performance increase is more than a quantitative step as certain investigations can only be performed with substantially higher flux and brightness. In 2005 the mission need for a facility enabling experiments with a spatial resolution of 1 nm and an energy resolution of 0.1 meV was recognized by the Department of Energy which marked the start of the NSLS-II project based on a 3 GeV electron storage ring. The mission need translates into demanding performance requirements for NSLS-II. The goal of the photon beam brightness is 10^{21} ·mm⁻²·mrad⁻²·s⁻¹·(0.1%BW)⁻¹ for 2 keV photons which implies beam currents of 500 mA and a horizontal beam emittance of less than 1π nm rad. The beam orbit has to be stabilized to 200 nm. Novel and cutting edge accelerator technology is needed to meet these ambitious goals.

STORAGE RING DESIGN

The small horizontal beam emittance of the storage ring is achieved with a large circumference of 792 m and with 30 double-bend-achromat cells. The soft bending field of $B = 0.4$ Tesla helps to design a lattice with a horizontal emittance close to the theoretical minimum without generating excessive chromaticity as the lattice functions for minimum emittance scale with the length of the dipole magnet. The other advantage of the soft bending field is the relatively low synchrotron radiation power emitted from the beam in the dipole magnets (the electron energy loss per turn is only 283 keV). This is exploited by adding 3 x 7 m of damping wigglers ($B_{\text{peak}} = 1.8$ Tesla, 100 mm

*Work performed under the auspices of U.S. Department of Energy, under contract DE-AC02-98CH10886

[#]willeke@bnl.gov

period) distributed over three dispersion free 9.3m long straight sections which reduces the horizontal radiation damping time by a factor of two leading to a reduction of the beam emittance from $\epsilon_x = 2$ nm to $\epsilon_x = 1$ nm. The small beam energy spread is thereby increased to a moderate 0.1%. Space for another 21 m of damping wigglers provides an option to further reduce the beam emittance. The DBA cell has a four quadrupoles and a sextupole triplet between the two dipoles and triplets on each side of the straight sections. Maximum β -functions are below 32 m, the absolute values of the natural chromaticity per cell are below 3. The lattice has alternating long ($L = 9.3$ m) and short ($L = 6.6$ m) straight sections for insertion devices with large ($\beta_x = 20$ m, $\beta_y = 3.8$ m) and small ($\beta_x = 1.8$ m, $\beta_y = 1.3$ m) values of beta respectively. The lattice functions are shown in Figure 1.

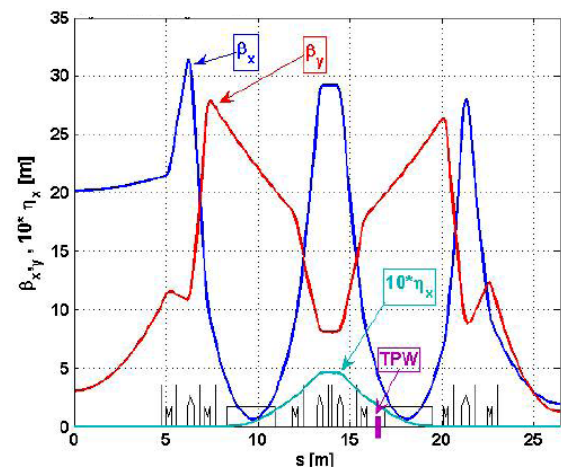


Figure 1: Lattice functions of the NSLS-II DBA structure.

The main beam parameters are listed in Table 1. One of the long straight sections is needed for injection and two are for the four superconducting single-cell 500 MHz cavities and the two passive superconducting 3rd harmonic cavities for reduction of peak intensity.

ACCELERATOR PHYSICS

Coulomb scattering of electrons in the bunch (Touschek Effect [2]) imposes a strong intensity dependent reduction of beam lifetime in NSLS-II which is mitigated by a large dynamic aperture. The highly optimized nine sextupole circuits per cell with three circuits for chromatic corrections provide a robust dynamic aperture of ± 15 mm horizontally and ± 3 mm vertically for particles with up to 3% energy deviation from nominal. The mirror symmetry of the achromat is broken by shifting one of the two defocusing sextupole magnets by 15 cm longitudinally which provides sufficient corrective strength for higher

order chromatic effects [3]. The Touschek-dominated beam lifetime for the design bunch current of 0.5 mA amounts to 3 hrs for bunches with a natural rms bunch length of 4.5 mm. Optimization of dynamic aperture is achieved by a systematic reduction of the driving terms of nonlinear resonances, of tune shift with amplitude and of chromaticity [4] as well as by employing a multi-objective approach [5]. While the baseline lattice has 15-fold symmetry, studies [6] have been carried out which suggest that 12 of the 15 long straight sections can be operated with small beta ($\beta_x=2$ m, $\beta_y=3$ m). This would make the up to 12 available long straight sections much more attractive for insertion devices.

As the beam current is allowed to vary by only 0.5%, NSLS-II is designed for and will be operated in Top-Off mode with injection of up to 10 nC per minute. The safety aspects of Top-Off injection have been addressed in a comprehensive study using an efficient cascading technique to make sure that charged particles cannot enter the photon extraction channels: the beam phase space envelope which is populated by test particles after transport through an element with a range of errors is repopulated uniformly for tracking through the following element. The corresponding reduction in computing time enables the detection of extremely rare trajectories and increases the reliability of the study considerably [7].

Table 1: Main Beam Parameters

Parameter	Unit	Value
Beam Energy	GeV	3
Beam Current	mA	500
H/V Beam	π -nm-rad	$> 0.7, 0.012$
Emittance		
Orbit stability	Nm	< 300
Beam Lifetime	Hr	> 3
Bunch spacing	Ns	2
Number of bunches	l	~ 1000
Circumference	M	792
Damping time (long)	Ms	37
Energy Spread	%	0.1
Bunch length	Mm	9-2
RF Power	kW	1240

INJECTOR

The NSLS-II injector [8] consists of a LINAC, a booster and two transfer lines. The 200 MeV S-band LINAC is fed by a thermionic gun, it has four 156 cell 3 GHz accelerating structures and a 500 MHz pre-buncher and 3 GHz pre-buncher and buncher systems. The klystron amplifiers are powered by solid state modulators which deliver 93 MW peak power. The linac can deliver up to 15 nC in a 300 ns long pulse train with a repetition rate of up to 10 Hz. A short pulse mode with 330 ps pulse length is supported as well. The LINAC is provided as a turn-key system by the manufacturer. The 158 m circumference combined function booster synchrotron, which is installed in a separate tunnel located on the

inside of the storage ring building accelerates up to 30 mA of electrons to 3 GeV for on-energy injection into the storage ring. The injection into the booster is on-axis. A transverse stacking option is considered to increase injection intensity, if needed [9]. The booster repetition frequency is 1 Hz, but components like vacuum, magnets, electrical infrastructure, and controls are laid out for a 2 Hz cycle. Injection into the storage ring is based on multi-turn injection with four kicker magnets which produce half sine-wave, two-turn long pulses. The beam is transported into the injection straight by the in-vacuum septum magnet.

INFRASTRUCTURE

For sufficient thermal stability, the temperature variation in the storage ring tunnel is limited to 0.1 !C. Air conditioning systems are built to meet this requirement. The storage ring tunnel is 3.7 m wide (most narrow section) and has a height of 3.2 m. The beam is 1.2 m above the tunnel floor and 1.4 m above the experimental floor. The experimental floor has a width of 17 m and is shielded from the tunnel by the 111 cm thick ratchet wall. In the injection areas, the wall is made from heavy concrete. The 81 cm strong tunnel roof forms a mezzanine used for installation of power-supplies, electronics and controls. Other equipment such as de-ionized water systems and the HVAC systems are located in the five service building distributed around inside of the ring. Figure 3 shows the footprint of the facility and figure 4 shows a cross section of the tunnel and the experimental floor.

TECHNICAL SUBSYSTEMS

For sufficient dynamic aperture, the 810 normal conducting dipole, quadrupole and sextupole magnets require very low relative field errors of $(1-10) \cdot 10^{-5}$ at 25mm radius. This requires manufacturing techniques such as wire erosion, high precision milling, or fine blanking to shape the poles with a precision of (5-10) microns [10].

The magnets are aligned within 30 micron precision on their support structures which required the development of a novel high precision stretched wire method to determine the centre of the magnets. The precision of this method of 5 microns has been demonstrated [11]. The support structure is designed for vibration frequencies > 30 Hz and high thermal stability with a requirement of better than 25 nm [12]. The feasibility of the technical implementation of high precision alignment and highly stable supports has been extensively tested and confirmed with prototype magnets and supports.

Setting up the accelerator for operation with ultra bright beams needs beyond the state of the art instrumentation. The heart of the diagnostic system is the beam position monitors system with required long term stability of 200 nm and a resolution of 200 nm. The system is based on narrow band pass architecture with sampling the 500 MHz signal at 116 MHz utilizing 16-bit ADCs. While

comparable systems are commercially available, an improved system based on Xilinx Virtex-6 FPGA processing and correction of long-term drift by inclusion of an out-of-band calibration tone was developed in-house. This is a significant improved of existing systems. The system is now fully developed. Beam tests at the Advanced Light Source at LBL confirm the design performance with 400 nm turn-by-turn resolution and 200 nm stability of 8 hrs [13].

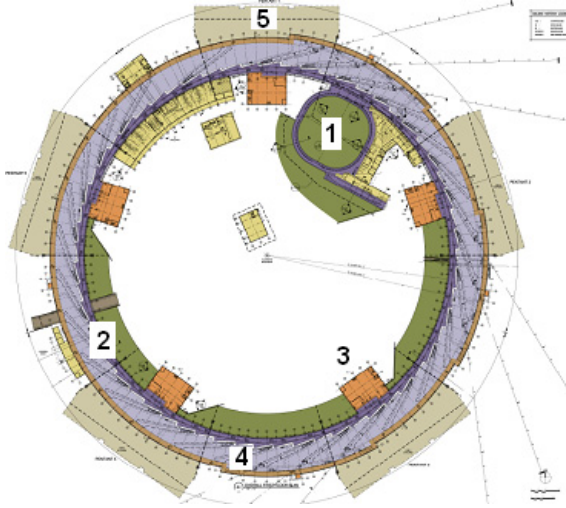


Figure 3: Footprint of NSLS-II showing the injector (1), the tunnel (1), the service buildings (3), the experimental floor (4), and five laboratory office buildings (5)

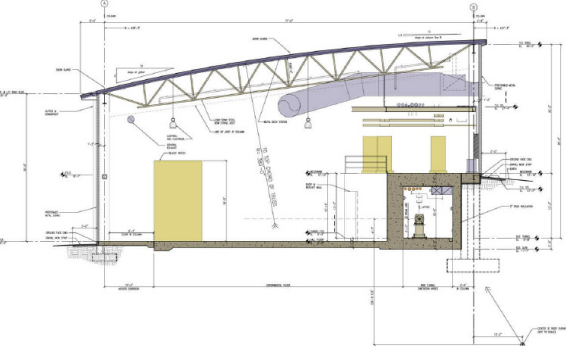


Figure 4: Cross section of NSLS-II

The vacuum system [14] is made from keyhole-shaped extruded aluminum with integrated NEG pumping. It is fully protected from synchrotron radiation emitted in the dipoles by a Glidcop absorber system. Protection of the vacuum system from undulator radiation requires an active interlock system.

The power supplies are all switched-mode with a precision and stability of better than 25 ppm. They are installed in sealed air-cooled racks. The protection from humidity, dust and large temperature gradients as well as the absence of direct water cooling is expected to provide MTBF values in the order of $5 \cdot 10^5$.

The NSLS-II controls are based on EPICS. A novel feature is the quasi deterministic shared memory bus with a data rate of 2.5Gbps connecting the 30 cell controllers

which provide quasi deterministic real time connectivity of BPMs, and fast correctors for fast orbit correction and for the machine protection system [15].

The required orbit stability is 10% of the beam size which is only 3 μm (vertical) in the middle of a straight section. This requires active feedback with high precision BPM readings at 10 kHz. The feedback is a distributed system with the correction algorithm integrated into the cell controllers. The built-up of DC offsets in the weak fast air coil correctors (3 per cell, 15 micro-radian maximum strength) is avoided by continuously adjusting the offsets of the DC correctors (6 per cell) in open loop fashion while the fast feedback is active and correcting for residuals. AC and DC correctors are driven by different controllers and power supplies. This concept provides a robust and stable correction system and avoids any band-gap issues between the fast and slow orbit correction systems [16].

To exploit the unique properties of the NSLS-II beam, state-of-the-art and beyond insertion devices are constructed. The NSLS-II damping wigglers are optimized for the purpose of increasing the radiation damping rates but they constitute at the same time a powerful source of hard X-rays which cover the spectral range up 100 keV.

The standard insertion device of the facility will be the in-vacuum undulator with 20 mm period and 6 mm gap (IVU20). The field of 1.12 T corresponds to a maximum K value of 1.81. There is a 1.5m long IVU with 21 mm period (IVU21) and a 3m long IVU with 22mm period (IVU22) in the baseline as well. Since the bending magnet has a low field, short three-pole wigglers with a strong center pole of $B=1$ T is foreseen to be installed upstream of the downstream bending magnets in the achromats. This provides a significant photon flux above 20 keV. The project scope also contains a canted pair of elliptically polarized undulators with 49mm period length. The spectral brightness of NSLS-II radiation sources is shown in figure 5.

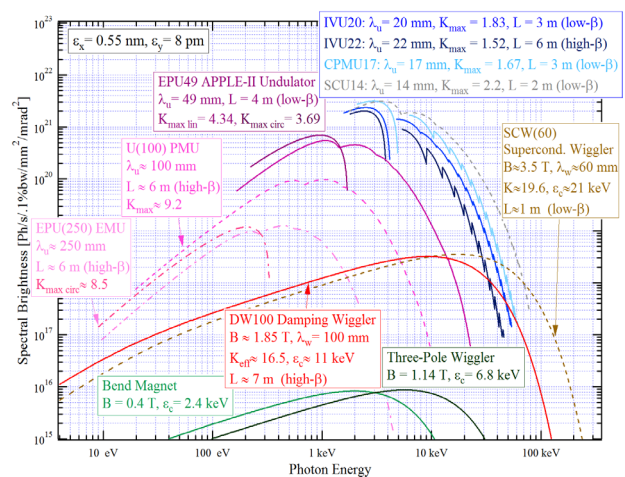


Figure 5: Brightness of NSLS-II radiation sources [17].

Cryogenically cooled devices are considered as well. R&D is underway to explore the feasibility of magnet arrays using novel bake-able Pr-Fe-B with excellent field stability which would allow a period of 17mm resulting in a factor of 2 in brilliance [18] (see figure 6).

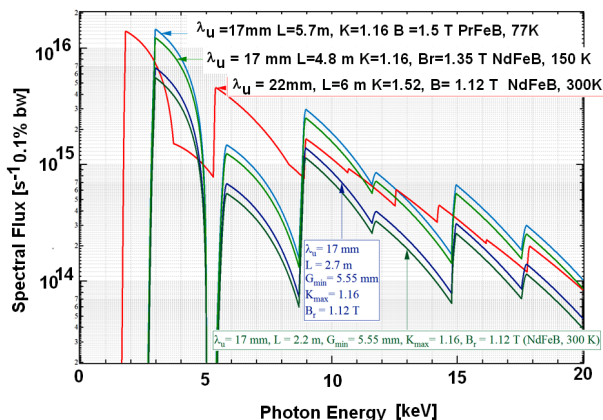


Figure 6: Comparison of spectral flux achieved for different technologies for NSLS-II in-vacuum-undulators. The cryogenically cooled Pr-Fe-B based design provides twice as many 9 keV photons as the room temperature Nd-Fe-B based design [18].

The RF system [19] consists of 2-4 superconducting, single cell 500MHz RF cavities, each driven by a 310 kW klystron amplifier. The 500 MHz superconducting cavities are of the CESR-B-type [20] which have been further developed to accommodate the latest cryogenic-vacuum safety regulations and are optimized for NSLS-II operating parameters. This re-optimization resulted in a thicker cavity resonator wall (3mm) and an optimized input coupler design. The 1-2 two-cell superconducting passive third harmonic cavities, which lengthen the 4.5 mm long bunch by a factor of two, are based on a new NSLS-II design. They are being developed and built in collaboration with industry.

BEAM LINES

NSLS-II will provide space for at least 60 beamlines. Six beamlines are funded by the NSLS-II project. The inelastic X-ray scattering beam line (IXS) is driven by the IVU22. It will operate at 9 keV photon energy and has a novel type of monochromator made of a sequence of asymmetrically cut single crystals (CDW monochromator) [21]. This provides an energy resolution of 0.1 meV. The 60 m long hard X-ray nanoprobe beamline, driven by an IVU20 is optimized for imaging with a spatial resolution of 1 nm. It extends to outside the ring building. The hard X-Ray powder diffraction beamline (XPD) is using the radiation from two 3.5m long damping wigglers. The coherent soft X-ray scattering beamline (CSX) is driven by the pair of canted elliptically polarized undulators and is specialized for the investigation of magnetic and anisotropic materials. SRX is a high resolution spectroscopy beam line driven by the

IVU21 undulator and the coherent X-hard X-ray scattering beam is driven by an IVU20. There are three additional beamlines which are already funded which are in the process of being defined. Present plans are to provide up to 21 further beamlines for NSLS-II start-up the progress of which will depend on available funding.

CONSTRUCTION STATUS

Civil construction of the facility is well advanced. The concrete and steel structure as well as the roof of the ring building has been completed (see figure 7). The first pentant is fully functional including heating and air conditioning and installation of the accelerator systems have already been started.



Figure 7: Birds-eye view of the far advanced NSLS-II ring building.

The orders for the large turn-key subsystems, the LINAC, the booster, the liquid Helium plant, and the RF transmitter systems have been placed. These systems are already in production. The integration of the vacuum system from extruded Aluminum is performed at BNL while extrusion and machining are provided by industry. The delicate welding is performed at the robotic welding facility and Argonne National Laboratory. At BNL, the NEG pumps are installed, the RF shield for suppressing higher order modes is inserted, the BPM buttons are mounted and the system is baked and conditioned for installation. This process is well underway. All extrusions are complete and about 30% of the 150 vacuum chambers are ready for installation. A large fraction of the vacuum pumps are already on hand and the valves and the instrumentation are well in production. The design of the shielded bellows and the synchrotron radiation absorbers was completed only recently and production is just starting. Many of accelerator subsystems such as BPM buttons, power supplies, electrical utilities, cooling water systems, and damping wigglers are in production at industrial manufacturers. The 810 storage ring magnets (seven types of quadrupoles, three types of sextupoles, two types of dipoles, three types of dipole correctors) are being produced at six different manufacturers. About 15% of the production is completed to date. The start-up of magnet production was a difficult and involved process which required the development of appropriate manufacturing and measurement procedures, in intense collaboration between manufacturers and NSLS-II engineers. The challenge is not only to consistently achieve the magnet field quality but also to construct the magnets such that the field quality is reliably reproducible

after the magnets are reassembled after separating the two halves of quadrupole and sextupole magnets. This is necessary to be able to install the vacuum chamber without loss of field quality. Once the vacuum chamber is installed, it is almost impossible to re-measure the field of the magnets and verify good field quality. Reproducibility tests with first article units have been performed for all production lines. The matured design and the highly optimized manufacturing process results in excellent field reproducibility. Figure 8 shows an example of field reproducibility of the 25 cm long quadrupole magnet with 68 mm pole radius and a gradient of 14 T/m.

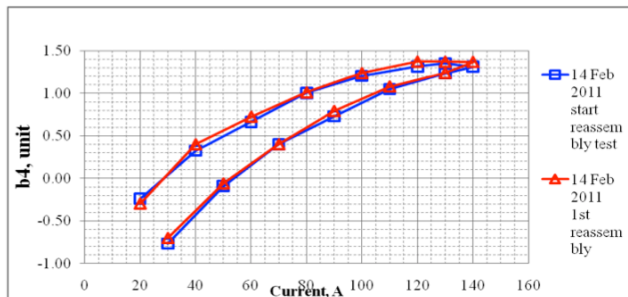


Figure 8: Reproducibility of field quality of NSLS-II short quadrupole magnet produced by Budker Institute of Nuclear Physics in Russia: Shown is the octupole component in units of 10^{-4} of the quadrupole field both taken at $r = 25$ mm as a function of excitation before (blue squares) and after (red triangles) magnet disassembly-reassembly.

Since March 2011, installation of accelerator components in the storage ring tunnel and on the mezzanine is in progress. The first step is the installation of the secondary survey network, of piping for the de-ionized water and of cable trays in the first pentant of the ring building. Starting in April, the power supply and instrumentation cables will be mounted. Meanwhile the first magnet girder has been completed including vacuum instrumentation and supports (see figure 9). Installation of the first pentant will be completed in September 2011. Installation of storage ring girders is planned to start by the end of April 2011.

The injector building will be available for installation in July 2011. The delivery of the LINAC is planned for late September with installation in October. The booster systems will be installed in summer 2012.

Meanwhile, preparation for commissioning of the NSLS-II accelerator chain has started. The commissioning of the LINAC is planned for the end of 2011. This will be followed by the commissioning of the booster synchrotron in the fall of 2012. Storage ring commissioning will start in May 2013 and will be completed in February 2014 which will mark the start-up of NSLS-II operations.

ACKNOWLEDGEMENT

The author would like to acknowledge the ingenuity and the commitment of the entire NSLS-II team which

has resulted in novel solutions for many of the challenging design and manufacturing problems and has enabled very good progress of the NSLS-II project.



Figure 9: First completed magnet-vacuum girder of the NSLS-II Storage ring carrying magnets, vacuum chamber, and beam instrumentation hardware, cooling manifolds, support systems and cable trays.

REFERENCES

- [1] NSLS-II Preliminary Design Report, <http://www.bnl.gov/nsls2/project/PDR/default.asp>
- [2] C. Bernardini, G. F. Corazza, G. Di Giugno, G. Ghigo, J. Haissinski, P. Marin, R. Querczoli, and B. Touschek, Phys. Rev. Lett. 10, 407 (1963).
- [3] W. Guo, Proc. PAC09., Vancouver (2009).
- [4] J. Bengtsson, "NSLS-II: Control of Dynamic Aperture", BNL-81770-2008-IR.
- [5] Lingyun Yang, WEP065, this conference.
- [6] F. Lin, THP189, this conference.
- [7] Y. Li et al, MOP276, this conference.
- [8] T. Shaftan, Proc. ICPAC10, WEP089, Kyoto (2010).
- [9] R. Fliller et al, WEP 283, this conference.
- [10] J. Skaritka et al, MO6PFP008, Proc. of PAC'09, Vancouver (2009).
- [11] A. Jain, et al., Proc. 10th Int. Workshop on Accel. Alignment, 2008, Tsukuba.
- [12] S. Sharma et al, THOBS2, this conference.
- [13] K. Vetter et al, MOP211, this conference.
- [14] H.C. Hseuh, TUP 227, this conference.
- [15] G. Carcassi et al, TUP104, Proc. ICALEPS (2009).
- [16] T. Yuke, WEODNY, this conference.
- [17] T. Tanabe et al, THOBS4, this conference.
- [18] O. Choubar, private comm.
- [19] J. Rose, "The NSLS-II RF System", this conference.
- [20] D. Moffat et al, Preparation and testing of a superconducting cavity for CESR-B, PAC (1993).
- [21] Yu.V. Shvyd'ko et al., Proc. 9th Internatl. Conf. Synchr. Rad. Instr. 2007, Vol 879, pp. 737-745 (2007).